Acyl chain orientational order in large unilamellar vesicles: comparison with multilamellar liposomes: a ^2H and ^{31}P nuclear magnetic resonance study

David B. Fenske and Pieter R. Cullis

Liposome Research Unit, Department of Biochemistry, Faculty of Medicine, University of British Columbia, Vancouver, British Columbia V6T 1Z3 Canada

ABSTRACT Large unilamellar vesicles (LUVs) composed of 1-[$^2H_{31}$]palmitoyl-2-oleoyl phosphatidylcholine (POPC-d_{31}), with diameters of ~117 ± 31 and 180 ± 44 nm, were prepared by extrusion through polycarbonate filters with pore sizes of 0.1 and 0.2 μm, respectively. The ^2H nuclear magnetic resonance (NMR) spectra obtained at 21°C contain two components: a broad component (~17 kHz linewidth) corresponding to the methylene groups and a narrower component originating from the methyl groups. Spectra with increasing powder pattern characteristics were obtained by reducing the rate of phospholipid reorientations by addition of glycerol (to increase the solvent viscosity) and by lowering the temperature. Full powder spectra, characteristic of liquid-crystalline bilayers, were obtained for both LUV samples at 0°C in the presence of 50 wt% glycerol. Individual quadrupolar splittings were not resolved in these spectra, due to broader linewidths in the LUVs, which have significantly shorter values for spin-spin relaxation time T_2 measured from the decay of the quadrupolar echo (90 μs) than the multilamellar vesicles (MLVs; 540 μs). Smoothed order parameter profiles (OPPs) were obtained for these samples by integration of the dePaked spectra. The OPPs were very similar to the OPP of POPC-d_{31} MLVs in 50 wt% glycerol at the same temperature, indicating that orientational order in MLVs and LUVs with a diameter of ≥100 nm is essentially the same. The presence of 80 wt% glycerol was found to have a disordering effect on the vesicles.

INTRODUCTION

Model membrane systems have played an important role in providing insight into the structure and function of biological membranes. Numerous model systems exist that have been used to address a wide variety of problems, ranging from the motional and structural properties of constituent lipids and/or proteins, to the barrier properties of the membrane as a whole. The most commonly used systems involve the lipid bilayer; these include oriented multibilayers (1), multilamellar dispersions (powder samples) (2), and unilamellar vesicles (3, 4). Much information has also been obtained from the study of nonbilayer polymorphic assemblies, such as the hexagonal H_{II}, cubic, and micellar phases that can be adopted by some phospho- and glycolipids under certain conditions (5–13).

The ability of phospholipids to form several bilayer models of differing morphology has led to questions concerning the validity of comparing data obtained from different model systems. One of the best-known examples of this has been the controversy surrounding the effect of curvature on the properties of bilayers. Early investigations into the properties of small unilamellar vesicles (SUVs),[1] prepared by sonication of multilamellar vesicles (MLVs), revealed that the high curvature of these vesicles altered their thermodynamic properties (14–16) and resulted in a profound packing asymmetry of the inner and outer monolayers (17–25). As many of these studies involved nuclear magnetic resonance (NMR) measurements, the question arose as to whether the orientational order of the lipid acyl chains in SUVs was the same as that in MLVs. The quantitative determination of order parameters in MLVs was made possible by the advent of ^2H NMR spectroscopy (2); large MLV samples give rise to broad-line spectra that result from partial anisotropic averaging of the quadrupolar interaction by local molecular motion. Each deuterium-labeled carbon in a lipid chain gives rise to a quadrupolar splitting, which is directly proportional to the order parameter S_{CD} for that carbon–deuterium bond. Unfortunately, this methodology was not directly applicable to SUVs, as their smaller size resulted in high-resolution spectra because of isotropic averaging of the quadrupolar interaction. This led to a controversy, which is still the focus of research, as to whether the narrow lines could be explained solely by isotropic tumbling of the vesicles and lateral diffusion of the lipids, or whether additional disorder, resulting from the higher curvature of the bilayers, must also be invoked. The former view was supported by results obtained from ^1H NMR (26–28), ^2H NMR (29), and ^{13}C NMR (30). However, a number of studies using ^1H NMR (31), ^{13}C NMR (32), and ^2H NMR (33) supported the latter view. Resolutions to this problem have recently been proposed, based on monolayer packing asymmetry (34) and motional averaging resulting from lateral diffusion over the vesicle inner monolayer (35), but it is not yet clear whether either of these solutions are valid. It is of interest that order parameters obtained from fluorescence depolarization (36) and ESR measurements (37) also support a reduction of order in SUVs.

Address correspondence to Dr. David B. Fenske, Department of Biochemistry, Faculty of Medicine, University of British Columbia, 2146 Health Sciences Mall, Vancouver, B.C. V6T 1Z3 Canada.

[1] *Abbreviations used in this paper:* LUV, large unilamellar vesicle; MLV, multilamellar vesicle; NMR, nuclear magnetic resonance; OPP, order parameter profile; POPC-d_{31}, 1-[$^2H_{31}$]palmitoyl-2-oleoyl phosphatidylcholine; SUV, small unilamellar vesicle; T_{2e}, spin-spin relaxation time T_2 measured from the decay of the quadrupolar echo.

0006-3495/93/05/1482/10 $2.00

Of the model systems mentioned above, MLVs have been widely utilized, especially in solid-state NMR studies, allowing elucidation of much information on lipid order and dynamics (2, 38–43). However, many topics of importance cannot be addressed using MLVs, and require the use of unilamellar vesicles. This applies particularly to investigations of the permeability properties of lipid bilayers, transbilayer lipid asymmetry, the generation and maintenance of ion or pH gradients, membrane fusion, and drug uptake. Furthermore, the unilamellar systems must be well defined with respect to lamellarity, size, and stability. However, it is clear from the discussion above that SUVs are not the ideal system for investigating such topics within a biophysical framework, especially for studies involving magnetic resonance techniques. Aside from the difficulty in quantifying such parameters as lipid order, one must consider the complications that may arise from the packing asymmetry of the two monolayers. Since the putative reduction in order and the monolayer asymmetry are due to the high curvature of SUVs, it would follow that these differences will be reduced as vesicle size increases, and that the use of LUVs should provide a system that more closely models the properties of MLVs. Unfortunately, this reasonable assumption has not yet been demonstrated using NMR, and it is not yet known at what size the effects of curvature become minimal, although it has been predicted, using geometrical arguments, that this will occur for vesicle diameters on the order of 100 nm (17). The purpose of the present paper, therefore, is to determine the ^{2}H NMR order parameter profiles (OPPs) of LUVs with diameters of ~100 and 200 nm, and compare them to the OPPs of MLVs (which have diameters in the micrometer range). The same methodology will be used in all cases, making comparisons meaningful. Inasmuch LUVs are widely used in the study of fundamental membrane processes such as permeability (44, 45), fusion (46, 47), and asymmetry (47–49), and within clinical settings for such purposes as drug delivery (50–52), a characterization of their properties by NMR seems useful and timely.

MATERIALS AND METHODS

1-[$^2H_{31}$]palmitoyl-2-oleoyl phosphatidylcholine (POPC-d_{31}) was obtained from Avanti Polar Lipids, Inc. (Birmingham, AL). Deuterium-depleted water was obtained from Sigma Chemical Co. (St. Louis, MO).

Multilamellar dispersions (MLVs) were prepared for NMR by hydrating the lipid with deuterium-depleted water (lipid concentration ~ 25 mg/ml), and cyclically heating above the gel to liquid–crystalline phase transition temperature with vortex mixing and freeze-thawing to homogeneity (typically five cycles). LUVs were prepared by extrusion as described by Hope et al. (4) using an extruder obtained from Lipex Biomembranes (Vancouver, BC, Canada). MLVs were subjected to 10 passes (under pressure) through two stacked polycarbonate filters of pore size 0.1 and 0.2 μm to give vesicle populations with mean diameters of ~100 and 200 nm, respectively.

^{2}H NMR spectra were acquired at 46 MHz on a home-built spectrometer, using the quadrupolar echo pulse sequence with quadrature detection, and phase cycling of all pulses (53). The ^{2}H $\pi/2$ pulse length was 4.0 μs (10-mm solenoid coil), the interpulse spacing τ was 30–50 μs, and the recycle time was 300 ms. Spectra were acquired with a dwell time of 2 or 5 μs, and between 10,000 and 200,000 transients were collected for signal averaging. T_{2e} values were obtained by measuring the decay of the quadrupolar echo intensity as a function of the interpulse spacing τ. In general, 14 spectra were acquired corresponding to τ values ranging from 30 to 600 μs. In a perdeuteriated sample such as POPC-d_{31}, a superposition of T_{2e} values, resulting from T_2 anisotropy across the spectrum and a superposition of spectra for each labeled position, will give rise to a nonexponential echo decay, and thus a semilog plot of echo intensity versus 2τ is nonlinear above τ values in the range of 70-100 μs. The cited T_{2e} values were obtained from the initial linear slope, and thus represent an average of the shortest T_{2e}s.

^{2}H NMR spectra were dePaked to give the 0° orientation spectra (i.e., the spectra that would be obtained for an oriented sample with the external magnetic field parallel to the bilayer normal), from which the smoothed OPPs were obtained as described (54, 55). Briefly, the innermost splitting is assigned directly to the methyl group. The remaining area of the dePaked spectrum is normalized to the remaining 28 deuterium nuclei, and divided into 14 equal areas corresponding to C2–C15 of the palmitoyl chain. A mean value of the order parameter is calculated for each unit area corresponding to a methylene group. A monotonic decrease in order from C2 to C16 is assumed, with the result that a smoothed OPP is obtained, meaning that small local variations in order, such as might originate from geometrical effects, will not be resolved. The method gives the general shape of the order gradient, as shown by a comparison of the order profile so obtained for POPC-d_{31} with discrete order parameter values obtained from selectively labeled POPC (55). The usefulness of the method stems from the fact that the order profile can be obtained from a single sample and does not require resolved splittings. An example of this is given by ^{2}H NMR spectra of hexagonal phase 1-palmitoyl-2-oleoyl phosphatidylethanolamine (POPE). Although the quadrupolar splittings are not resolved in the dePaked spectra, the smoothed OPPs were obtained and compared with the profiles of bilayer phase lipid (54, 56).

The integration and dePaking procedures do not calculate uncertainties or errors. However, an estimate of the uncertainties can be obtained in two ways. Both sides of the dePaked spectra are integrated separately, and the total integral is given. In all cases, the differences were <5%. A second method is to compare the variation in quadrupolar splittings obtained from the two sides of the dePaked spectrum. This gives a maximum variation in S_{CD} of ±0.006, giving uncertainties in the range of 1–5%. For MLVs, the uncertainties were slightly smaller, in the range of 0–2%.

^{31}P NMR spectra were acquired at 81.0 MHz on a spectrometer (model MSL-200; Bruker Instruments, Inc., Billerica, MA) using a Hahn echo pulse sequence (57) with WALTZ decoupling (gated on during acquisition). The ^{31}P $\pi/2$ pulse length was 4.0 μs (10-mm solenoid coil), the interpulse spacing was 60 μs, and the recycle time was 5.0 s.

The mean diameters of the LUVs were determined by using a submicron particle sizer (model 270; Nicomp Instruments, Santa Barbara, CA). The scattering angle was 90°, the channel width was 10 μs, and the autocorrelation function was evaluated over 64 channels. The results are expressed as mean diameters ± standard deviation.

RESULTS AND DISCUSSION

The present study represents an initial characterization of the physical properties of LUVs by comparing the orientational OPPs of LUVs with those of MLVs. Smoothed OPPs are obtained from MLVs via dePaking of the ^{2}H NMR powder pattern followed by integration of the dePaked spectrum as described by Sternin et al. (54) and Lafleur et al. (55). However, extraction of order parameters from vesicle samples is not as straight-

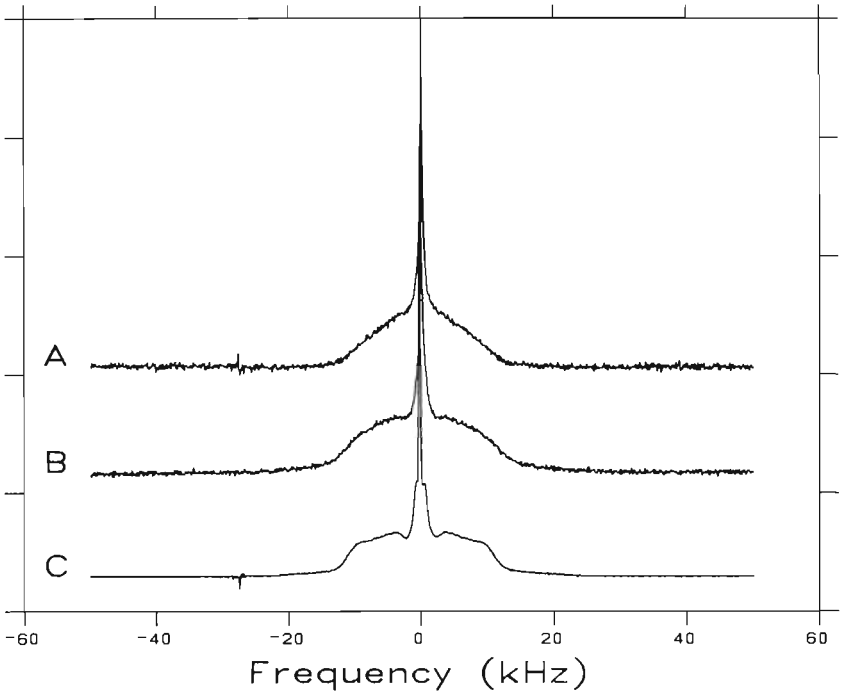

FIGURE 1 ^{2}H NMR spectrum of POPC-d_{31} LUVs (diameter, 117 nm) acquired at 21°C in the presence of 0 (*A*), 50 (*B*), and 80 (*C*) wt% glycerol.

forward. For vesicles in the extreme narrowing regime, such as SUVs (diameter, 20 nm), which give high-resolution Lorentzian spectra, a straightforward equation describes the relationship between order parameters and ^{2}H NMR linewidths (29). Quantitative use of this equation requires both fatty acyl chains that are deuteriated at only a single position and knowledge of the vesicle size distribution (33). Unfortunately, order parameters cannot be obtained in such a manner from the linewidths of LUVs. The approach described by Stockton et al. (29) is valid only when the correlation time for vesicle reorientation, τ_e, is much less than $(e^2qQ/h)^{-1}$, where (e^2qQ/h) is the quadrupolar coupling constant (168 kHz). While this holds for SUVs, τ_e for LUVs with a diameter of 100 nm is $\sim 3 \times 10^{-5}$ s, whereas $(e^2qQ/h)^{-1} = 5.8 \times 10^{-6}$ s. LUVs are in the intermediate motional regime, where complete averaging of the quadrupolar interaction does not occur (29). This can be seen in Fig. 1 *A*, which shows the ^{2}H NMR spectrum of POPC-d_{31} LUVs prepared by extrusion through polycarbonate filters with a pore size of 0.1 μm. The mean diameter determined by QELS was 117 ± 31 nm. Two components are apparent in the spectrum, a broad symmetric lineshape with a linewidth of ~17 kHz, originating from the methylene resonances, and a narrow line that contains contributions mainly from the terminal methyl groups. The linewidth of the broad component is 30 times greater than observed in SUVs (33). If the size distribution of these LUVs was known, the motional narrowing theory of Freed and co-workers (58) could be used to generate theoretical lineshapes for vesicles of various OPPs. A more direct approach is to reduce the rate of phospholipid reorientations so that the powder lineshape, and thus the OPP, can be observed directly. Isotropic averaging of the static powder lineshape occurs via particle tumbling and lipid lateral diffusion; the rates of these processes are described by the correlation times τ_t and τ_d, respectively. The effective correlation time τ_e for phospholipid reorientations is thus given by (28):

$$1/\tau_e = 1/\tau_t + 1/\tau_d \quad (1)$$

where

$$\tau_t = 4\pi\eta R^3/3kT \quad (2)$$

$$\tau_d = R^2/6D, \quad (3)$$

where D is the translational diffusion coefficient for the lateral diffusion of phospholipid in the plane of the bilayer, η is the solvent viscosity, k is the Boltzmann constant, and R is the vesicle radius. In addition, the lipid lateral diffusion coefficient may be sensitive to the viscosity of the surrounding medium according to (59):

$$D = [kT/(4\pi\eta' h)][\log(\eta' h/\eta r) - \gamma], \quad (4)$$

where η' is the viscosity of the membrane, h and r are the height and radius, respectively, of the lipid molecule modeled as a cylinder, and γ is a constant. It is clear from these equations that both vesicle tumbling and lateral diffusion will be sensitive to changes in solvent viscosity and temperature, and, additionally, the rate of lateral diffusion will also depend on the membrane viscosity. With respect to the validity of Eq. 4, it is worth noting

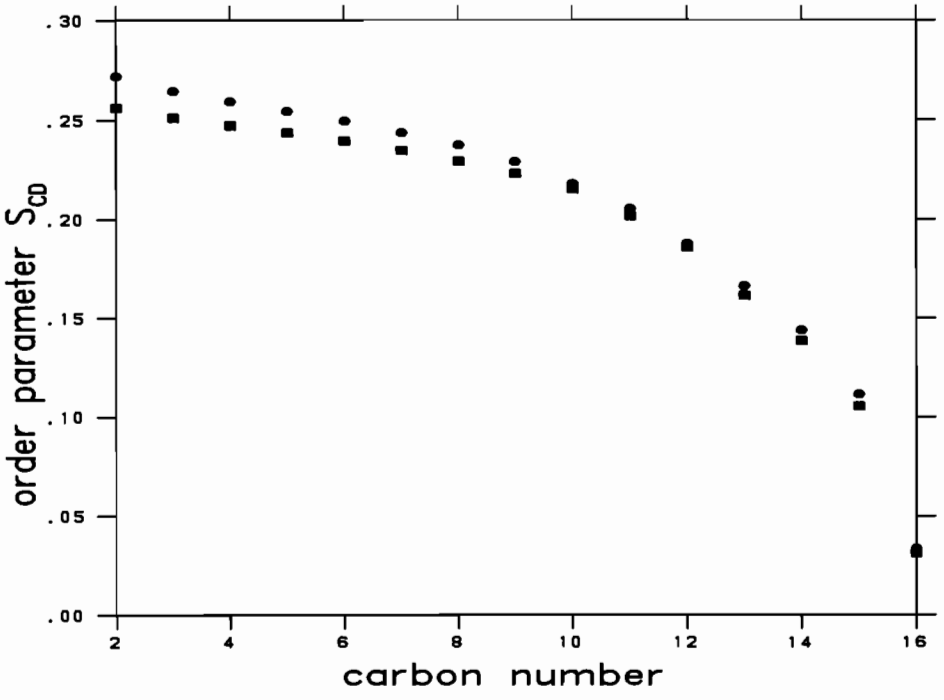

FIGURE 2 Smoothed OPPs obtained from POPC-d_{31} MLVs at 0°C in the absence (*circles*) and presence (*squares*) of 50 wt% glycerol.

that a value of $D = 4 \times 10^{-8}$ cm^2/s was calculated for POPC MLVs in water at 30°C, in good agreement with the value of 5×10^{-8} cm^2/s estimated for POPC 800 nm MLVs (M. Monck, unpublished results) and for other phospholipids (60) using two-dimensional ^{31}P NMR, and with estimates of D obtained by other NMR techniques (see reference 61). Although we will use the results obtained from Eqs. 1–4 in a qualitative manner only, as a number of assumptions are involved in the derivation of Eq. 4 (see reference 62), and a number of the parameters are only known approximately (e.g., the membrane viscosity), we will find that they are useful in understanding the NMR lineshapes obtained at different temperatures in the presence of glycerol.

Initially, the solvent viscosity was regulated by the addition of glycerol to the sample. Previous studies using ^{31}P NMR have established that glycerol has little effect on vesicle structure (62, 63). Glycerol concentrations up to 60 wt% have little effect on the main transition temperatures and enthalpies of dipalmitoylphosphatidylcholine (DPPC) MLVs (64), and concentrations of 3 M have no effect on the leakage rates of carboxyfluorescein from egg phosphatidylcholine (PC) vesicles (65). To assess the effect of glycerol on membrane order, spectra of POPC-d_{31} MLVs in water and in 50% glycerol were obtained at 0°C. In both cases the spectra (not shown) were axially symmetric, indicative of membranes in the liquid–crystalline phase; the smoothed OPPs are plotted in Fig. 2. The presence of glycerol does result in a slight disordering of the plateau region (C2–C9) of <10%, but this effect is small, and the general shape of the OPP is unaffected. The effect of increasing concentrations of glycerol on the ^{2}H NMR lineshape of 117 nm LUVs at 21°C is shown in Fig. 1, *B* and *C*. As the proportion of glycerol is increased from 0 to 50 wt% (Fig. 1 *B*) to 80 wt% (Fig. 1 *C*), the lineshape develops partially averaged powder characteristics. However, even at 80 wt% glycerol, averaging of the static powder lineshape is evident. At 20°C in water, for vesicles with a radius of 5.85 nm, $\tau_t = 2.1 \times 10^{-4}$ s and $\tau_d = 1.2 \times 10^{-4}$ s (Eqs. 1–3, assuming $D = 5 \times 10^{-8}$ cm^2/s). Thus, lateral diffusion is the dominant line-narrowing mechanism under these conditions. Using Eqs. 1–3, we predict only a 1.5-fold increase in τ_e as the solvent viscosity is increased from 1 cP (water) to 60 cP (80% glycerol). However, if Eq. 4 is included in the calculation, i.e., if allowance is made for the effect of solvent viscosity on lateral diffusion, then τ_e increases fivefold as the viscosity is increased (assuming a membrane viscosity of 1 P). Thus, the observed significant change in lineshape in Fig. 1 suggests that lateral diffusion is reduced by the high concentrations of glycerol, although not sufficient to prevent some residual averaging. The same trends are also observed for LUVs prepared by extrusion through filters with a 0.2-μm pore size (Fig. 3), that have a mean diameter of 180 ± 44 nm as determined by quasi-elastic light scattering (QELS). Although the larger 180-nm LUVs have a slower reorientation rate, the lineshapes still display significant motional averaging in the presence of glycerol at 21°C.

To further reduce vesicle reorientations, the glycerol-containing samples were cooled to 0°C, ~7°C above the gel to liquid–crystalline phase transition of the lipid.

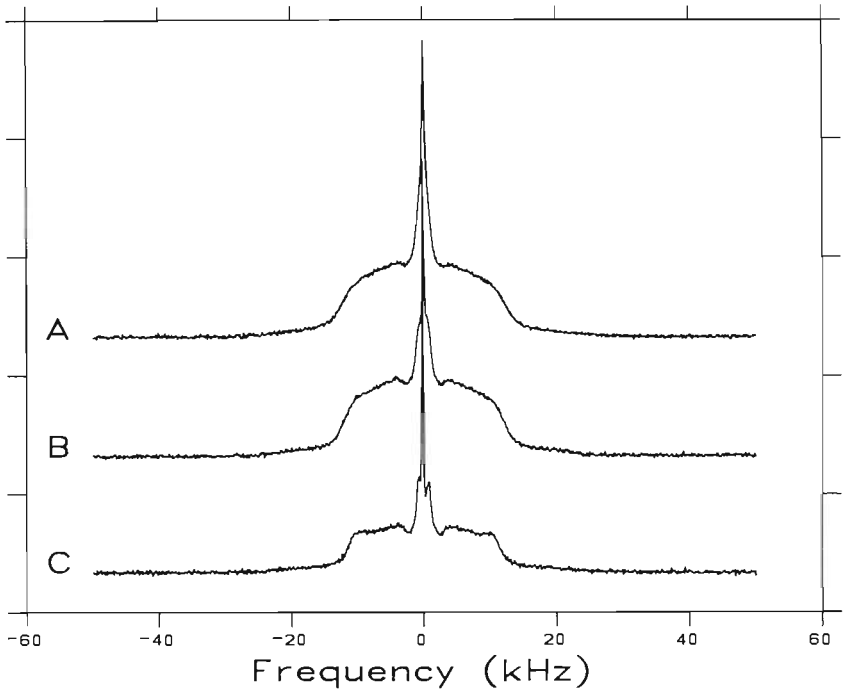

FIGURE 3 ^2H NMR spectrum of POPC-d_{31} LUVs (diameter, ~180 nm) acquired at 21°C in the presence of 0 (*A*), 50 (*B*), and 80 (*C*) wt% glycerol.

This will result in an increase in the solvent viscosity η and the membrane viscosity η', both of which will reduce the lipid diffusion rate. At 0°C, the viscosity of 50% glycerol is ~0.15 Poise. The most common technique used for estimating membrane viscosity is fluorescence polarization (66–68). A decrease in temperature results in a significant increase in membrane viscosity, from <1 Poise at 40°C to ~10 P at 0°C (67). The values reported at low temperature span a wide range, from 2.4 Poise for egg lecithin at 10°C (66) to 12.3 Poise for a phospholipid mixture (approximating the composition of erythrocytes) at 4°C (68). If we assume a reasonable value of 10 P for POPC at 0°C, then in the presence of 50 wt% glycerol, the diffusion rate will be reduced by an order of magnitude, giving τ_c values in the range of 1 and 3 ms for LUVs with diameters of 117 and 180 nm, respectively. In MLVs, estimates of correlation times for phospholipid reorientations obtained by one-dimensional "holeburning" (69) and two-dimensional NMR methods (60, 70, 71) range from 8 to 40 ms. Thus, the combination of increasing the solvent viscosity and reducing the temperature to 0°C results in a reduction in the rate of phospholipid reorientations in LUVs to the timescale regime of MLVs.

Spectra obtained for the 117- and 180-nm LUVs in 50 wt% glycerol at 0°C are shown in Fig. 4, *B* and *C*, respectively. The spectrum for POPC-d_{31} MLVs at the same temperature in 50 wt% glycerol is shown in Fig. 4 *A*. The LUV spectra have the same width and general shape as the MLV spectrum, indicating similar lipid order and minimal residual averaging due to vesicle rotation and lipid lateral diffusion. The individual methylene resonances for C10–C15 are not resolved in the LUV spectra; this is at least partly due to T_2 differences. Measurements of T_{2e} were obtained for the LUV and MLV samples, as described in Materials and Methods, at 0°C in the presence of 50 wt% glycerol. Values of 85, 92, and 540 μs were obtained for the 117-nm LUV, 180-nm LUV, and MLV samples, respectively. The shorter LUV T_{2e} values will result in broader linewidths in the spectra and a loss of resolution. One possible source of the reduced T_{2e} is lateral diffusion over the vesicle surface (42, 72). The LUV spectra are similar to those observed with spherical support vesicles (diameter 1.5 μm), single bilayers supported on glass beads with a narrow, well-defined size distribution (73). The loss of resolution in these systems has also been partially attributed to the significantly shorter transverse relaxation times obtained for spherical support vesicles (74).

To obtain a quantitative comparison of order in the MLV and LUV samples, the spectra in Fig. 4 were de-Paked to give the 0° orientation spectra, and the smoothed order profiles were obtained as described (54, 55). This methodology gives the general shape of the order profile, and allows the entire order profile to be obtained from one (perdeuterated) sample, thereby removing the costly and time-consuming exercise of preparing many selectively labeled samples. The usefulness of this approach has been demonstrated in both model (54, 55) and biological (75) systems. In the present case, the OPPs obtained for MLVs and LUVs (117 and 180 nm) at 0°C in 50 wt% glycerol are plotted in Fig. 5 (*top*

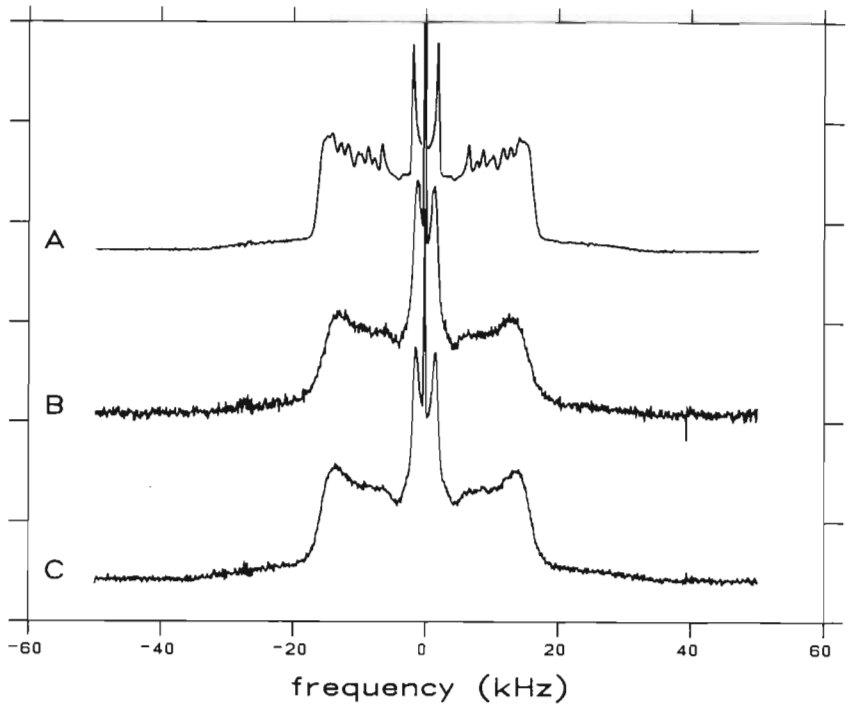

FIGURE 4 ^{2}H NMR spectra of POPC-d_{31} MLVs (*A*) and LUVs with diameters of ~117 (*B*) and 180 nm (*C*), at 0°C, in the presence of 50 wt% glycerol.

curve; open and *closed circles* and *closed squares*). It is clear that these profiles are very similar, with the order parameters at each position falling within a fairly narrow range, aside from a slight difference between LUV and MLV observed at C2. The OPPs of the MLVs and LUVs differ by only 1–3% for most positions, particularly those

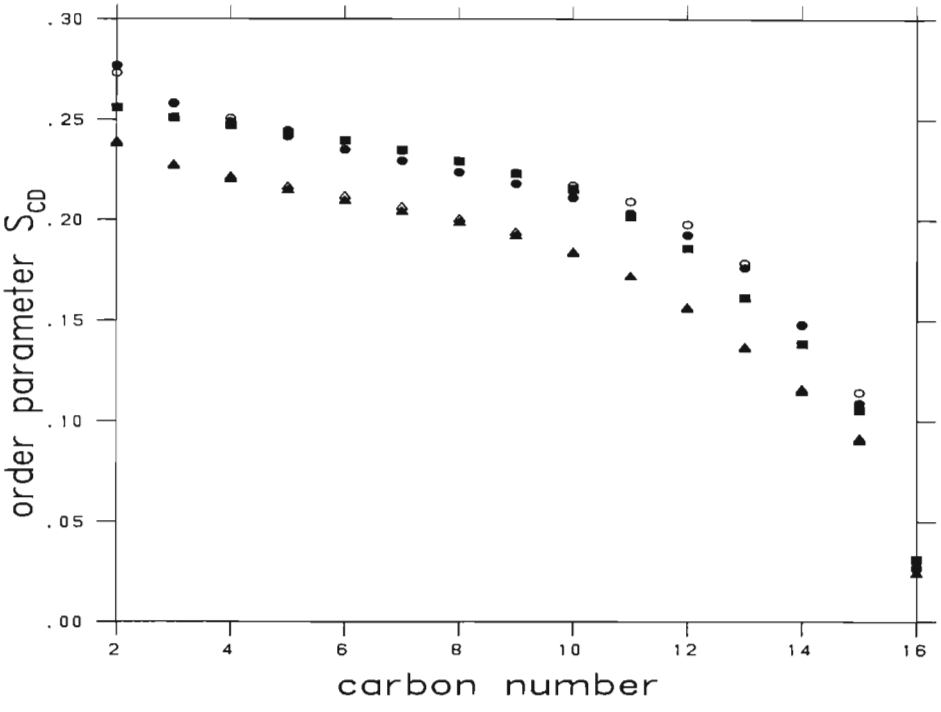

FIGURE 5 Smoothed OPPs obtained from the spectra in Figs. 4 and 6. The top curve corresponds to MLVs (*squares*), 117-nm LUVs (*closed circles*), and 180-nm LUVs (*open circles*) in the presence of 50 wt% glycerol. The bottom curve corresponds to 117-nm LUVs (*closed triangles*) and 180-nm LUVs (*open triangles*) in the presence of 80 wt% glycerol.

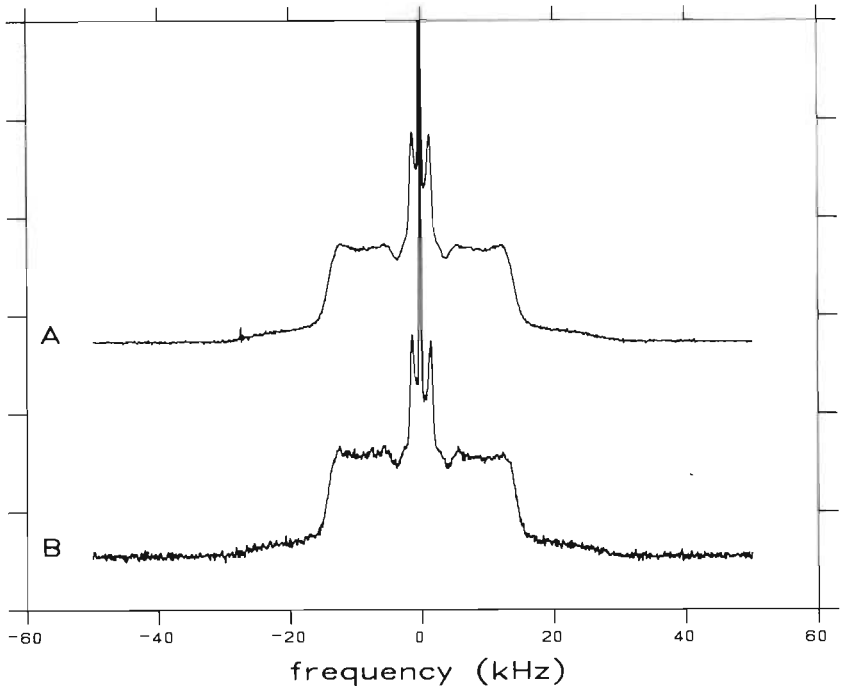

FIGURE 6 ^{2}H NMR spectra of POPC-d_{31} LUVs with diameters of ~117 nm (*A*) and 180 nm (*B*), at 0°C, in the presence of 80 wt% glycerol.

in the plateau region. This is less than the estimated uncertainty in S_{CD} of <5% (see Materials and Methods). More variation is observed between the MLVs and LUVs for positions 11–15 (8–10%), but these differences are small compared with the twofold reduction in order reported by some workers for SUVs (33), or with the large changes in order that result from the addition of cholesterol (76). This demonstrates that orientational order is not significantly altered by curvature for vesicles with diameters of ≥100 nm, a conclusion consistent with early theoretical predictions (17).

The spectra obtained for the LUVs in 80 wt% glycerol at 0°C are shown in Fig. 6. The spectra are narrower and have a "flatter" profile than those obtained in 50 wt% glycerol. Thus, it would appear that the perturbing effects of glycerol become more severe at higher concentrations. The OPPs obtained from these spectra are reduced over the entire length of the acyl chain (Fig. 5, *bottom curve, open* and *closed triangles*). Nevertheless, it is clear from these results as well that the OPPs of the 117- and 180-nm LUVs are identical.

For purposes of comparison, ^{31}P NMR spectra were obtained for the same samples under identical conditions, and the results are shown in Fig. 7. The results from the 117-nm LUVs are shown in the left column, and those of the 180-nm LUVs in the right column. The bottom spectrum in the left column corresponds to MLVs in 50% glycerol at 0°C. The same trends are observed as with the ^{2}H spectra, i.e., the combination of the addition of glycerol and reduction in temperature results in powder-like lineshapes. However, on the basis of the spectra acquired at 0°C, the LUVs do not appear to be as immobile as they do from the equivalent ^{2}H spectra; a greater degree of motional averaging is apparent in the ^{31}P spectra. This observation can be understood from consideration of the greater width of the ^{2}H spectra. Complete averaging of broadline NMR spectra occurs when the motions are much faster than the reciprocal of the width of the spectrum, in frequency units. For ^{2}H, with quadrupolar splittings in the range of 30 kHz, the correlation time for molecular motion must be $<3 \times 10^{-5}$ s for complete averaging. For ^{31}P, where $\Delta\sigma$ values are ~3,500 Hz at 81 MHz, the correlation time need only be $<3 \times 10^{-4}$ s. Thus, for LUVs, ^{31}P spectra will be more sensitive to partial averaging by slow reorientations than will ^{2}H spectra. It should be noted that the ^{31}P spectra of LUVs in 50 and 80% glycerol at 0°C are similar; thus, the narrowing observed in the ^{2}H spectra can be attributed to disordering rather than a morphological change induced by the high concentrations of glycerol.

Conclusions

In the present study, smoothed OPPs were derived for MLVs and LUVs prepared from POPC-d_{31}. The use of glycerol at low temperatures to slow vesicle reorientation allowed the LUV powder pattern lineshape to be observed directly, removing the need for spectral simulations, and the assumptions inherent in such simulations. The effect of glycerol on MLV order was minimal (<10%) up to a concentration of ~50 wt%; the presence of 50 wt% glycerol in both MLV and LUV samples allowed the order profiles obtained from both sample types to be compared directly. Both the magnitude of the order parameters at each carbon and the shape of the

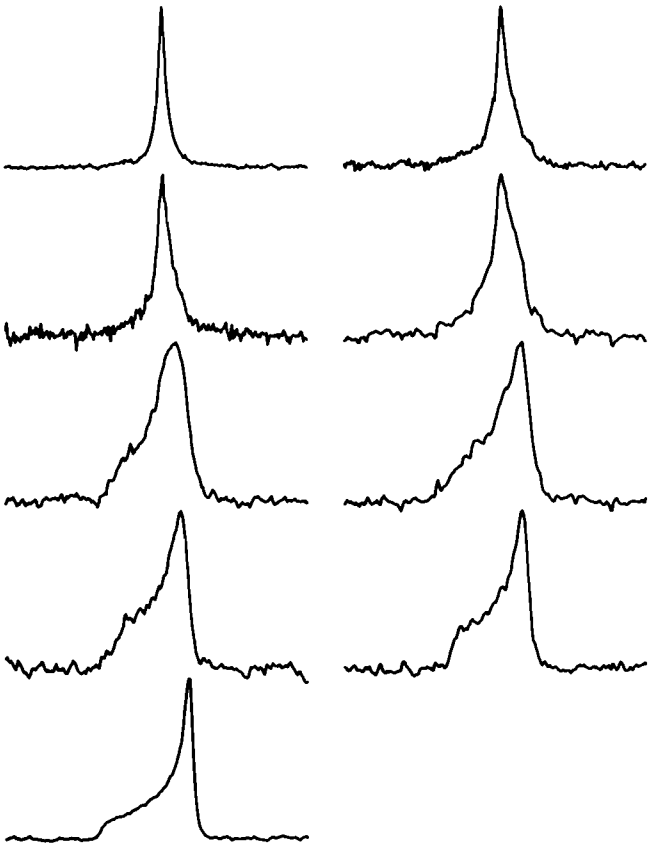

FIGURE 7 ^{31}P NMR spectra of LUVs with diameters of ~117 nm (*left*) and 180 nm (*right*), and of MLVs in 50% glycerol at 0°C (*left, bottom*). The experimental conditions for the LUV samples were (*top* to *bottom*) water at 21°C, 50% glycerol at 21°C, 50% glycerol at 0°C, 80% glycerol at 0°C. The plot width is 12 kHz.

order profiles were very similar for MLVs and LUVs with diameters > 100 nm. Thus vesicle curvature has little effect on lipid order for radii as small as 50 nm, meaning that comparable information can be derived from results obtained with LUVs in this size range and from results obtained with MLVs.

We thank Professor Myer Bloom for the use of his ^{2}H NMR facilities. We are grateful to Myrna Monck for helpful discussions, and acknowledge the technical assistance of Kakoli Mitra.

This work was supported by the Medical Research Council of Canada.

Received for publication 19 November 1992 and in final form 20 January 1993.

REFERENCES

1. Jarrell, H. C., P. A. Jovall, J. B. Giziewicz, L. A. Turner, and I. C. P. Smith. 1987. Determination of conformational properties of glycolipid head groups by ^{2}H NMR of oriented multibilayers. *Biochemistry.* 26:1805–1811.
2. Seelig, J. 1977. Deuterium magnetic resonance: theory and applications to lipid membranes. *Q. Rev. Biophys.* 10:353–418.
3. Finer, E. G., A. G. Flook, and H. Hauser. 1972. Mechanism of sonication of aqueous egg yolk lecithin dispersions and nature of the resultant particles. *Biochim. Biophys. Acta.* 260:49–58.
4. Hope, M. J., M. B. Bally, G. Webb, and P. R. Cullis. 1985. Production of large unilamellar vesicles by a rapid extrusion procedure. Characterization of size distribution, trapped volume and ability to maintain a membrane potential. *Biochim. Biophys. Acta.* 812:55–65.
5. Cullis, P. R., and B. de Kruijff. 1979. Lipid polymorphism and the functional roles of lipids in biological membranes. *Biochim. Biophys. Acta.* 559:399–420.
6. Lindblom, G., and L. Rilfors. 1989. Cubic phases and isotropic structures formed by membrane lipids—possible biological relevance. *Biochim. Biophys. Acta.* 988:221–256.
7. Seddon, J. M. 1990. Structure of the inverted hexagonal (H_{II}) phase, and non-lamellar phase transitions of lipids. *Biochim. Biophys. Acta.* 1031:1–69.
8. Siegel, D. P. 1984. Inverted micellar structures in bilayer membranes. *Biophys. J.* 45:399–420.
9. Siegel, D. P. 1986. Inverted micellar intermediates and the transitions between lamellar, cubic, and inverted hexagonal lipid phases. I. Mechanism of the $L_{\alpha} * H_{II}$ phase transitions. *Biophys. J.* 49:1155–1170.
10. Siegel, D. P. 1986. Inverted micellar intermediates and the transitions between lamellar, cubic, and inverted hexagonal lipid phases. II. Implications for membrane–membrane interactions and membrane fusion. *Biophys. J.* 49:1171–1183.
11. Siegel, D. P. 1986. Inverted micellar intermediates and the transitions between lamellar, cubic, and inverted hexagonal amphiphile phases. III. Isotropic and inverted cubic state formation via intermediates in transitions between L_{α} and H_{II} phases. *Chem. Phys. Lipids.* 42:279–301.
12. Siegel, D. P., J. L. Burns, M. H. Chestnut, and Y. Talmon. 1989. Intermediates in membrane fusion and bilayer/nonbilayer phase transitions imaged by time-resolved cryo-transmission electron microscopy. *Biophys. J.* 56:161–169.
13. Fenske, D. B., and P. R. Cullis. 1992. Chemical exchange between lamellar and non-lamellar lipid phases. A one- and two-dimensional ^{31}P-NMR study. *Biochim. Biophys. Acta.* 1108:201–209.
14. Gruenewald, B., S. Stankowski, and A. Blume. 1979. Curvature influence on the cooperativity and the phase transition enthalpy of lecithin vesicles. *FEBS (Fed. Eur. Biochem. Soc.) Lett.* 102:227–229.
15. Suurkuusk, J., B. R. Lentz, Y. Barenholz, R. L. Biltonen, and T. E. Thompson. 1976. A calorimetric and fluorescent probe study of the gel–liquid crystalline phase transition in small, single-lamellar dipalmitoylphosphatidylcholine vesicles. *Biochemistry.* 15:1393–1401.
16. Lentz, B. R., Y. Barenholz, and T. E. Thompson. 1976. Fluorescence depolarization studies of phase transitions and fluidity in phospholipid bilayers. 1. Single component phosphatidylcholine liposomes. *Biochemistry.* 15:4521–4528.
17. Sheetz, M. P., and S. I. Chan. 1972. Effect of sonication on the structure of lecithin bilayers. *Biochemistry.* 11:4573–4581.
18. Berden, J. A., P. R. Cullis, D. I. Hoult, A. C. McLaughlin, G. K. Radda, and R. E. Richards. 1974. Frequency dependence of ^{31}P NMR linewidths in sonicated phospholipid vesicles: effects of chemical shift anisotropy. *FEBS (Fed. Eur. Biochem. Soc.) Lett.* 46:55–58.
19. Longmuir, K. J., and F. W. Dahlquist. 1976. Direct spectroscopic observation of inner and outer hydrocarbon chains of lipid bilayer vesicles. *Proc. Natl. Acad. Sci. USA.* 73:2716–2719.
20. Chrzeszczyk, A., A. Wishnia, and C. S. Springer, Jr. 1977. The

intrinsic structural asymmetry of highly curved phospholipid bilayer membranes. *Biochim. Biophys. Acta.* 470:161–169.

21. Huang, C., and J. T. Mason. 1978. Geometric packing constraints in egg phosphatidylcholine vesicles. *Proc. Natl. Acad. Sci. USA.* 75:308–310.
22. Eigenberg, K. E., and S. I. Chan. 1980. The effect of surface curvature on the head-group structure and phase transition properties of phospholipid bilayer vesicles. *Biochim. Biophys. Acta.* 599:330–335.
23. Schuh, J. R., U. Banerjee, L. Muller, and S. I. Chan. 1982. The phospholipid packing arrangement in small bilayer vesicles as revealed by proton magnetic resonance studies at 500 MHz. *Biochim. Biophys. Acta.* 687:219–225.
24. Wu, W.-G., S. R. Dowd, V. Simplaceanu, Z.-Y. Peng, and C. Ho. 1985. ^{19}F NMR investigation of molecular motion and packing in sonicated phospholipid vesicles. *Biochemistry.* 24:7153–7161.
25. Tauskela, J. S., and M. Thompson. 1992. A ^{31}P-NMR spin-lattice relaxation and $^{31}P\{^1H\}$ nuclear overhauser effect study of sonicated small unilamellar phosphatidylcholine vesicles. *Biochim. Biophys. Acta.* 1104:137–146.
26. Finer, E. G., A. G. Flook, and H. Hauser. 1972. The nature and origin of the NMR spectrum of unsonicated and sonicated aqueous egg yolk lecithin dispersions. *Biochim. Biophys. Acta.* 260:59–69.
27. Finer, E. G. 1974. Calculation of molecular motional correlation times from linewidths in nuclear magnetic resonance spectra of aggregated systems. Effect of particle size on spectra of phospholipid dispersions. *J. Magn. Reson.* 13:76–86.
28. Bloom, M., E. E. Burnell, A. L. MacKay, C. P. Nichol, M. I. Valic, and G. Weeks. 1978. Fatty acyl chain order in lecithin model membranes determined from proton magnetic resonance. *Biochemistry.* 17:5750–5762.
29. Stockton, G. W., C. F. Polnaszek, A. P. Tulloch, F. Hasan, and I. C. P. Smith. 1976. Molecular motion and order in single-bilayer vesicles and multilamellar dispersions of egg lecithin and lecithin–cholesterol mixtures. A deuterium nuclear magnetic resonance study of specifically labelled lipids. *Biochemistry.* 15:954–966.
30. Lepore, L. S., J. F. Ellena, and D. S. Cafiso. 1992. Comparison of the lipid acyl chain dynamics between small and large unilamellar vesicles. *Biophys. J.* 61:767–775.
31. Bocian, D. F., and S. I. Chan. 1978. NMR studies of membrane structure and dynamics. *Annu. Rev. Phys. Chem.* 29:307–335.
32. Fuson, M. M., and J. H. Prestegard. 1983. Dynamics of fatty acids in phospholipid vesicles using spin relaxation of proton-coupled carbon-13 spectra. *J. Am. Chem. Soc.* 105:168–176.
33. Parmar, Y. I., S. R. Wassall, and R. J. Cushley. 1984. Orientational order in phospholipid bilayers. ^2H NMR study of selectively deuterated palmitic acids in unilamellar vesicles. *J. Am. Chem. Soc.* 106:2434–2435.
34. Wu, W.-G., S.-W. Leu, C.-H. Hsieh, and L.-M. Chi. 1991. The order of phosphatidylcholine head-group in sonicated cholesterol/phospholipid vesicles as revealed by ^1H-NMR. *Chem. Phys. Lipids.* 58:241–248.
35. Halle, B. 1991. ^2H NMR relaxation in phospholipid bilayers. Toward a consistent molecular interpretation. *J. Phys. Chem.* 95:6724–6733.
36. Kintanar, A., A. C. Kunwar, and E. Oldfield. 1986. Deuterium nuclear magnetic resonance spectroscopic study of the fluorescent probe diphenylhexatriene in model membrane systems. *Biochemistry.* 25:6517–6524.
37. Korstanje, L. J., E. E. van Faassen, and Y. K. Levine. 1989. Reorientational dynamics in lipid vesicles and liposomes studied with ESR: effects of hydration, curvature and unsaturation. *Biochim. Biophys. Acta.* 982:196–204.
38. Seelig, J. 1978. ^{31}P nuclear magnetic resonance and the head group structure of phospholipids in membranes. *Biochim. Biophys. Acta.* 515:105–140.
39. Griffin, R. G. 1981. Solid state nuclear magnetic resonance in lipid bilayers. *Methods Enzymol.* 72:108–174.
40. Davis, J. H. 1983. The description of membrane lipid conformation, order and dynamics by ^2H NMR. *Biochim. Biophys. Acta.* 737:117–171.
41. Bloom, M., and I. C. P. Smith. 1985. Manifestations of lipid–protein interactions in deuterium NMR. *In* Progress in Protein–Lipid Interactions. A. Watts and J. J. H. H. M. Depont, editors. Elsevier North Holland Biomedical Press, Amsterdam. 61–88.
42. Bloom, M., E. Evans, and O. G. Mouritsen. 1991. Physical properties of the fluid lipid-bilayer component of cell membranes: a perspective. *Q. Rev. Biophys.* 24:293–397.
43. Dufourc, E. J., C. Mayer, J. Stohrer, G. Althoff, and G. Kothe. 1992. Dynamics of phosphate head groups in biomembranes. Comprehensive analysis using phosphorus-31 nuclear magnetic resonance lineshape and relaxation time measurements. *Biophys. J.* 61:42–57.
44. Andrasko, J., and S. Forsen. 1974. NMR study of rapid water diffusion across lipid bilayers in dipalmitoyl lecithin vesicles. *Biochem. Biophys. Res. Commun.* 60:813–819.
45. Koenig, S. H., Q. F. Ahkong, R. D. Brown III, M. Lafleur, M. Spiller, E. Unger, and C. Tilcock. 1992. Permeability of liposomal membranes to water: results from the magnetic field dependence of T_1 of solvent protons in suspensions of vesicles with entrapped paramagnetic ions. *Magn. Reson. Med.* 23:275–286.
46. Prestegard, J. H., and M. P. O'Brien. 1987. Membrane and vesicle fusion. *Annu. Rev. Phys. Chem.* 38:383–411.
47. Eastman, S. J., M. J. Hope, K. F. Wong, and P. R. Cullis. 1992. Influence of phospholipid asymmetry on fusion between large unilamellar vesicles. *Biochemistry.* 31:4262–4268.
48. Redelmeier, T. E., M. J. Hope, and P. R. Cullis. 1990. On the mechanism of transbilayer transport of phosphatidylglycerol in response to transbilayer pH gradients. *Biochemistry.* 29:3046–3053.
49. Eastman, S. J., M. J. Hope, and P. R. Cullis. 1991. Transbilayer transport of phosphatidic acid in response to transmembrane pH gradients. *Biochemistry.* 30:1740–1745.
50. Ostro, M. J., and P. R. Cullis. 1989. Use of liposomes as injectable-drug delivery systems. *Am. J. Hosp. Pharm.* 46:1576–1587.
51. Cullis, P. R., L. D. Mayer, M. B. Bally, T. D. Madden, and M. J. Hope. 1989. Generating and loading of liposomal systems for drug-delivery applications. *Adv. Drug Delivery Rev.* 3:267–282.
52. Mayer, L. D., M. B. Bally, and P. R. Cullis. 1990. Strategies for optimizing liposomal doxorubicin. *J. Liposome Res.* 1:463–480.
53. Sternin, E. 1985. Data acquisition and processing: a systems approach. *Rev. Sci. Instrum.* 56:2043–2049.
54. Sternin, E., B. Fine, M. Bloom, C. P. S. Tilcock, K. F. Wong, and P. R. Cullis. 1988. Acyl chain orientational order in the hexagonal H_{II} phase of phospholipid-water dispersions. *Biophys. J.* 54:689–694.
55. Lafleur, M., B. Fine, E. Sternin, P. R. Cullis, and M. Bloom. 1989. Smoothed orientational order profiles of lipid bilayers by ^2H-nuclear magnetic resonance. *Biophys. J.* 56:1037–1041.
56. Lafleur, M., P. R. Cullis, B. Fine, and M. Bloom. 1990. Compari-

son of the orientational order of lipid chains in the L_α and H_{II} phases. *Biochemistry.* 29:8325–8333.

57. Rance, M., and R. A. Byrd. 1983. Obtaining high-fidelity spin-1/2 powder spectra in anisotropic media: phase-cycled Hahn echo spectroscopy. *J. Magn. Reson.* 52:221–240.
58. Freed, J. H., G. V. Bruno, and C. F. Polnaszek. 1971. Electron spin resonance lineshapes and saturation in the slow motional regime. *J. Phys. Chem.* 75:3385–3399.
59. Saffman, P. G., and M. Delbruck. 1975. Brownian motion in biological membranes. *Proc. Natl. Acad. Sci. USA.* 72:3111–3113.
60. Fenske, D. B., and H. C. Jarrell. 1991. Phosphorus-31 two-dimensional solid-state exchange NMR. Application to model membrane and biological systems. *Biophys. J.* 59:55–69.
61. Mackay, A. L., E. E. Burnell, C. P. Nichol, G. Weeks, M. Bloom, and M. I. Valic. 1978. Effect of viscosity on the width of the methylene proton magnetic resonance line in sonicated phospholipid bilayer vesicles. *FEBS (Fed. Eur. Biochem. Soc.) Lett.* 88:97–100.
62. Cullis, P. R. 1976. Lateral diffusion rates of phosphatidylcholine in vesicle membranes: effects of cholesterol and hydrocarbon phase transitions. *FEBS (Fed. Eur. Biochem. Soc.) Lett.* 70:223–228.
63. Burnell, E. E., P. R. Cullis, and B. De Kruijff. 1980. Effects of tumbling and lateral diffusion on phosphatidylcholine model membrane ^{31}P-NMR lineshapes. *Biochim. Biophys. Acta.* 603:63–69.
64. McDaniel, R. V., T. J. McIntosh, and S. A. Simon. 1983. Nonelectrolyte substitution for water in phosphatidylcholine bilayers. *Biochim. Biophys. Acta.* 731:97–108.
65. Anchordoguy, T. J., J. F. Carpenter, C. A. Cecchini, J. H. Crowe, and L. M. Crowe. 1990. Effects of protein perturbants on phospholipid bilayers. *Arch. Biochem. Biophys.* 283:356–361.
66. Cogan, U., M. Shinitzky, G. Weber, and T. Nishida. 1973. Microviscosity and order in the hydrocarbon region of phospholipid and phospholipid–cholesterol dispersions determined with fluorescent probes. *Biochemistry.* 12:521–528.
67. Shinitzky, M., and Y. Barenholz. 1978. Fluidity parameters of lipid regions determined by fluorescence polarization. *Biochim. Biophys. Acta.* 515:367–394.
68. Shinitzky, M., and M. Inbar. 1976. Microviscosity parameters and protein mobility in biological membranes. *Biochim. Biophys. Acta.* 433:133–149.
69. Larsen, D. W., J. G. Boylan, and B. R. Cole. 1987. Axially symmetric ^{31}P NMR lineshapes with selective excitation in the presence of lateral diffusion on a curved surface. *J. Phys. Chem.* 91:5631–5634.
70. Auger, M., I. C. P. Smith, and H. C. Jarrell. 1991. Slow motions in lipid bilayers. Direct detection by two-dimensional solid-state deuterium nuclear magnetic resonance. *Biophys. J.* 59:31–38.
71. Fenske, D. B., M. Letellier, R. Roy, I. C. P. Smith, and H. C. Jarrell. 1991. Effect of calcium on the dynamic behaviour of sialylglycerolipids and phospholipids in mixed model membranes. A ^{2}H and ^{31}P NMR study. *Biochemistry.* 30:10542–10550.
72. Bloom, M., and E. Sternin. 1987. Transverse nuclear spin relaxation in phospholipid bilayer membranes. *Biochemistry.* 26:2101–2105.
73. Bayerl, T. M., and M. Bloom. 1990. Physical properties of single phospholipid bilayers adsorbed to micro glass beads. *Biophys. J.* 58:357–362.
74. Brumm, T., A. Mops, C. Dolainsky, S. Bruckner, and T. M. Bayerl. 1992. Macroscopic orientation effects in broadline NMR-spectra of model membranes at high magnetic field strength. A method preventing such effects. *Biophys. J.* 61:1018–1024.
75. Monck, M. A., M. Bloom, M. Lafleur, R. N. A. H. Lewis, R. N. McElhaney, and P. R. Cullis. 1992. Influence of lipid composition on the orientational order in *Acholeplasma laidlawii* strain B membranes: a deuterium NMR study. *Biochemistry.* 31:10037–10043.
76. Lafleur, M., P. R. Cullis, and M. Bloom. 1990. Modulation of the orientational order profile of the lipid acyl chain in the L_α phase. *Eur. Biophys. J.* 19:55–62.